Conformal and covariant formulation of the Z4 system with constraint-violation damping

Daniela Alic,[1] Carles Bona-Casas,[2,3] Carles Bona,[2] Luciano Rezzolla,[1,4] and Carlos Palenzuela[5,4]

[1]*Max-Planck-Institut für Gravitationsphysik, Albert-Einstein-Institut, Potsdam-Golm, Germany*
[2]*Institute for Applied Computation with Community Code (IAC^3) Departament de Fisica,*
Universitat de les Illes Balears, 07122 Palma de Mallorca, Spain
[3]*Instituut voor Informatica, Universiteit van Amsterdam, 1098 XH Amsterdam, The Netherlands*
[4]*Department of Physics and Astronomy, Louisiana State University, Baton Rouge, Louisiana, USA*
[5]*Canadian Institute for Theoretical Astrophysics, Toronto, Ontario M5S 3H8, Canada*

We present a new formulation of the Einstein equations based on a conformal and traceless decomposition of the covariant form of the Z4 system. This formulation combines the advantages of a conformal decomposition, such as the one used in the BSSNOK formulation (i.e. well-tested hyperbolic gauges, no need for excision, robustness to imperfect boundary conditions) with the advantages of a constraint-damped formulation, such as the generalized harmonic one (i.e. exponential decay of constraint violations when these are produced). We validate the new set of equations through standard tests and by evolving binary black hole systems. Overall, the new conformal formulation leads to a better behavior of the constraint equations and a rapid suppression of the violations when they occur. The changes necessary to implement the new conformal formulation in standard BSSNOK codes are very small as are the additional computational costs.

I. INTRODUCTION

Numerical relativity has seen, over the last few years, a truly remarkable development. Starting from the first simulations showing that black-hole binaries could be evolved for a few orbits [1–3], or that black holes could be produced from unstable stellar configurations using simple gauges and without excision [4], new results have been obtained steadily. As a result, it is now possible to simulate binary black holes [5] and binary neutron stars [6] accurately for dozens of orbits, from the weak-field inspiral, down to the final black-hole ringdown (see also [7,8] for recent reviews on binary black holes and neutron stars, respectively). In addition, the progress in numerical relativity has also been accompanied by a comparable progress of analytical approximation techniques, which have been shown to be able to reproduce the numerical results to very high precision both for binary black holes [9,10] and for binary neutron stars [11]. Finally, numerical simulations have now investigated scenarios never considered before and that could lead to a new and deeper understanding of the astrophysics of compact objects [12,13].

There are several reasons behind this rapid progress, and the use of more accurate numerical techniques and the availability of larger computational facilities are certainly among the most important ones. None of these, however, would be useful without the use of formulations of the Einstein equations that are well-suited for numerical evolutions. Most of the present three-dimensional (3D) numerical-relativity codes implement either one of the two formulations discussed below. The first and most popular one is the conformal and traceless reformulation of the 3 + 1 ADM equations [14], which is also known as

the BSSNOK (or BSSN) formulation [15–17]. The second formulation is instead based on the use of a fully 4D form of the Einstein equations in coordinates that resemble the harmonic ones and is therefore known as the Generalized-Harmonic formulation (GH) [18].

There are several differences between these two formulations, each having its own advantages and disadvantages. One of the main advantages of BSSNOK is that, being based on a conformal decomposition, it can separate potential singular terms in the conformal factor. In addition, it can count on well-tested and robust gauge conditions, such as the singularity-avoiding slicing conditions of the 1 + log family [19]. Similarly, the spatial gauges can rely on the hyperbolic Gamma-driver condition for the shift vector [20] (or some recent variants for unequal-mass binaries [21–23]), which removes to a large extent, the gauge dynamics near the compact objects. When combined, these two gauge choices eliminate the need to excise a region of the computation domain inside the apparent horizon, greatly simplifying the numerical infrastructure. Finally, the use of the momentum constraint equations (but not of the energy constraint) in the evolution of the dynamical variables, which is crucial for ensuring strong hyperbolicity, provides BSSNOK with a certain "forgiveness", so that the violation of the constraints does not grow rapidly, even when boundary conditions which are constraint-violating are used near the strong-field region.

In contrast, the GH formulation uses a generalized harmonic gauge which cannot deal with the physical singularity inside the apparent horizon. As a result, at least for the gauges considered so far (see also [24,25]), it requires the use of excision and thus of numerical techniques that

are devised for handling a special region of the computational domain [26]. To its advantage, however, the GH formulation leads to a set of equations whose principal parts are wave equations and thus with very well-known mathematical properties. In addition, the use of damping terms allows for the dynamical control of the constraint violations and thus for a powerful way of reducing them when necessary. Of course, a solution with smaller constraint violations will intrinsically be a more accurate solution to the Einstein equations.

Clearly, it would be useful to employ a formulation of the Einstein equations that combines the best of both worlds and thus that has the robustness and gauge conditions of the BSSNOK formulation but, at the same time, has well-defined mathematical properties and the possibility of dynamically controlling the constraint violations as the GH formulation. As we will show, these properties are met by a new conformal and covariant formulation of the Z4 system with constraint-violation damping. This is obtained by starting from the fully covariant Z4 formulation [27] and by performing a conformal decomposition which includes *all* the nonprincipal terms coming from the covariant form of the equations. In addition, damping terms are included for controlling the constraints in the spirit of the GH formulation. We will refer to this new formulation as the conformal and covariant Z4 system, i.e. CCZ4, and present tests of its behavior by considering evolutions in vacuum of gauge waves in 1D and isolated and binary black holes in 3D.

It should be remarked that this is not the first time that a conformal decomposition of the Z4 system has been proposed and indeed a very interesting attempt has been made in Ref. [28], where it was named Z4c. Although the tests presented in Ref. [28] were performed in spherical symmetry, they already highlighted the potential of a conformal formulation of the Z4 system, especially in the presence of matter (see also [29,30]). Unfortunately, we were not able to obtain equally good results when evolving the formulation of Ref. [28] in vacuum and in 3D; at the same time, we did not find that our CCZ4 formulation is more sensitive to boundary problems than the BSSNOK one (this was a point raised in Ref. [28]).

The structure of the paper is as follows. In Sec. II, we derive the full set of the CCZ4 equations starting from the covariant form of the Z4 system. In Sec. III we introduce the details of the numerical infrastructure and present a numerical comparison between the CCZ4 and the BSSNOK systems for a gauge-wave test and for binary black-hole simulations. Finally, the conclusions are summarized in Sec. IV.

II. THE CONFORMAL COVARIANT Z4 SYSTEM

The Z4 formulation was introduced as a covariant extension of the Einstein equations [27], where the original elliptic constraints are converted into algebraic conditions

for a new four-vector Z_μ. This formulation can be derived from the covariant Lagrangian

$$\mathcal{L} = g^{\mu\nu}[R_{\mu\nu} + 2\nabla_\mu Z_\nu], \tag{1}$$

by means of a Palatini-type variational principle [31]. The vector Z_μ measures the deviation from the Einstein field equations. The algebraic constraints $Z_\mu = 0$ amount therefore to the fulfilling of the standard energy-momentum constraints. In order to control these constraints, the original system was supplemented with damping terms such that the true Einstein solutions (i.e. the ones satisfying the constraints) become an attractor of the enlarged set of solutions of the Z4 system [32]. The Z4 damped formalism can be written in covariant form as

$$R_{\mu\nu} + \nabla_\mu Z_\nu + \nabla_\nu Z_\mu + \kappa_1[n_\mu Z_\nu + n_\nu Z_\mu$$
$$- (1 + \kappa_2)g_{\mu\nu}n_\sigma Z^\sigma] = 8\pi\left(T_{\mu\nu} - \frac{1}{2}g_{\mu\nu}T\right), \tag{2}$$

where n_μ is the unit normal to the time slicing, $T_{\mu\nu}$ the stress-energy tensor and T its trace, i.e. $T \equiv g_{\mu\nu}T^{\mu\nu}$. The (constant) coefficients κ_i are free parameters related to the characteristic time of the exponential damping of constraint violations. Assuming energy-momentum tensor conservation, the Bianchi identities lead to the constraint-propagation system

$$\nabla^\nu\nabla_\nu Z_\mu + R_{\mu\nu}Z^\nu = -\kappa_1\nabla^\nu[n_\mu Z_\nu + n_\nu Z_\mu + \kappa_2 g_{\mu\nu}n_\sigma Z^\sigma]. \tag{3}$$

It has been shown in Ref. [32] that all the constraint-related modes are damped when

$$\kappa_1 > 0 \qquad \kappa_2 > -1. \tag{4}$$

The Z4 formulation can be rewritten as a Cauchy problem by performing the $3 + 1$ decomposition of the spacetime, in which the line element reads

$$ds^2 = -\alpha^2 dt^2 + \gamma_{ij}(dx^i + \beta^i dt)(dx^j + \beta^j dt), \tag{5}$$

where α is the lapse function, β^i is the shift vector and γ_{ij} the intrinsic metric of the constant-time slices. The Einstein equations within this decomposition lead to the well-known ADM system [14], which is usually cast as a system of evolution equations for the extrinsic curvature K_{ij} and the three-metric γ_{ij}, plus four elliptic equations for the energy (or Hamiltonian) and the momentum constraints, involving space derivatives of the dynamical fields γ_{ij} and K_{ij}. In the Z4 formulation, the energy-momentum constraints become evolution equations for Z_μ, modifying the principal part of the ADM system and converting it from weakly to strongly hyperbolic [33]. The $3 + 1$ decomposition of the Z4 formulation including the damping terms reads

$$(\partial_t - \mathcal{L}_\beta)\gamma_{ij} = -2\alpha K_{ij}, \tag{6}$$

$$(\partial_t - \mathcal{L}_\beta)K_{ij} = -\nabla_i\alpha_j + \alpha[R_{ij} + \nabla_iZ_j + \nabla_jZ_i - 2K_i^lK_{lj}$$
$$+ (K - 2\Theta)K_{ij} - \kappa_1(1 + \kappa_2)\Theta\gamma_{ij}]$$
$$- 8\pi\alpha\left[S_{ij} - \frac{1}{2}(S - \tau)\gamma_{ij}\right], \quad (7)$$

$$(\partial_t - \mathcal{L}_\beta)\Theta = \frac{\alpha}{2}\left[R + 2\nabla_jZ^j + (K - 2\Theta)K - K^{ij}K_{ij}\right.$$
$$\left. - 2\frac{Z^j\alpha_j}{\alpha} - 2\kappa_1(2 + \kappa_2)\Theta - 16\pi\tau\right], \quad (8)$$

$$(\partial_t - \mathcal{L}_\beta)Z_i = \alpha\left[\nabla_j(K_i^j - \delta_i^jK) + \partial_i\Theta - 2K_i^jZ_j\right.$$
$$\left. - \Theta\frac{\alpha_i}{\alpha} - \kappa_1Z_i - 8\pi S_i\right], \quad (9)$$

where $\mathcal{L}_\beta$ is the Lie derivative along the shift vector $\vec{\beta}$, Θ is the projection of the Z4 four-vector along the normal direction, $\Theta \equiv n_\mu Z^\mu = \alpha Z^0$, and the following definitions apply for matter-related quantities $\tau \equiv n_\mu n_\nu T^{\mu\nu}$, $S_i \equiv n_\nu T_i^\nu$, $S_{ij} \equiv T_{ij}$.

Equations (6)–(9) must be complemented with suitable gauge conditions that determine the system of coordinates used during the evolution. Of all the possible options, the most interesting ones are those which preserve the hyperbolicity of the full evolution system, such as the 1 + log family and the Gamma-driver shift condition.

As a first step towards deriving the CCZ4 formulation, we express the metric γ_{ij} in terms of a conformal metric $\tilde{\gamma}_{ij} = \phi^2\gamma_{ij}$ with unit determinant $\phi = (\det(\gamma_{ij}))^{-1/6}$, while the extrinsic curvature K_{ij} is decomposed into its trace $K \equiv K_{ij}\gamma^{ij}$ and in its trace-free components

$$\tilde{A}_{ij} = \phi^2\left(K_{ij} - \frac{1}{3}K\gamma_{ij}\right). \quad (10)$$

This allows us to write the three-dimensional Ricci tensor as $R_{ij} = \tilde{R}_{ij} + \tilde{R}_{ij}^\phi$, thus splitting it into a part containing conformal terms and another one containing space derivatives of the conformal metric

$$\tilde{R}_{ij} = -\frac{1}{2}\tilde{\gamma}^{lm}\partial_l\partial_m\tilde{\gamma}_{ij} + \tilde{\gamma}_{k(i}\partial_{j)}\tilde{\Gamma}^k + \tilde{\Gamma}^k\tilde{\Gamma}_{(ij)k}$$
$$+ \tilde{\gamma}^{lm}[2\tilde{\Gamma}_{l(i}^k\tilde{\Gamma}_{j)km} + \tilde{\Gamma}_{im}^k\tilde{\Gamma}_{kjl}], \quad (11)$$

$$\tilde{R}_{ij}^\phi = \frac{1}{\phi^2}[\phi(\tilde{\nabla}_i\tilde{\nabla}_j\phi + \tilde{\gamma}_{ij}\tilde{\nabla}^l\tilde{\nabla}_l\phi) - 2\tilde{\gamma}_{ij}\tilde{\nabla}^l\phi\tilde{\nabla}_l\phi], \quad (12)$$

where

$$\tilde{\Gamma}^i \equiv \tilde{\gamma}^{jk}\tilde{\Gamma}_{jk}^i = \tilde{\gamma}^{ij}\tilde{\gamma}^{kl}\partial_l\tilde{\gamma}_{jk}. \quad (13)$$

The conformal and covariant Z4 formulation (CCZ4) is thus given by the following system of evolution equations

$$\partial_t\tilde{\gamma}_{ij} = -2\alpha\tilde{A}_{ij}^{TF} + 2\tilde{\gamma}_{k(i}\partial_{j)}\beta^k - \frac{2}{3}\tilde{\gamma}_{ij}\partial_k\beta^k + \beta^k\partial_k\tilde{\gamma}_{ij}, \quad (14)$$

$$\partial_t\tilde{A}_{ij} = \phi^2[-\nabla_i\nabla_j\alpha + \alpha(R_{ij} + \nabla_iZ_j + \nabla_jZ_i - 8\pi S_{ij})]^{TF}$$
$$+ \alpha\tilde{A}_{ij}(K - 2\Theta) - 2\alpha\tilde{A}_{il}\tilde{A}_j^l + 2\tilde{A}_{k(i}\partial_{j)}\beta^k$$
$$- \frac{2}{3}\tilde{A}_{ij}\partial_k\beta^k + \beta^k\partial_k\tilde{A}_{ij}, \quad (15)$$

$$\partial_t\phi = \frac{1}{3}\alpha\phi K - \frac{1}{3}\phi\partial_k\beta^k + \beta^k\partial_k\phi, \quad (16)$$

$$\partial_t K = -\nabla^i\nabla_i\alpha + \alpha(R + 2\nabla_iZ^i + K^2 - 2\Theta K)$$
$$+ \beta^j\partial_jK - 3\alpha\kappa_1(1 + \kappa_2)\Theta + 4\pi\alpha(S - 3\tau), \quad (17)$$

$$\partial_t\Theta = \frac{1}{2}\alpha\left(R + 2\nabla_iZ^i - \tilde{A}_{ij}\tilde{A}^{ij} + \frac{2}{3}K^2 - 2\Theta K\right)$$
$$- Z^i\partial_i\alpha + \beta^k\partial_k\Theta - \alpha\kappa_1(2 + \kappa_2)\Theta - 8\pi\alpha\tau, \quad (18)$$

$$\partial_t\hat{\Gamma}^i = 2\alpha\left(\tilde{\Gamma}_{jk}^i\tilde{A}^{jk} - 3\tilde{A}^{ij}\frac{\partial_j\phi}{\phi} - \frac{2}{3}\tilde{\gamma}^{ij}\partial_jK\right)$$
$$+ 2\tilde{\gamma}^{ki}\left(\alpha\partial_k\Theta - \Theta\partial_k\alpha - \frac{2}{3}\alpha KZ_k\right) - 2\tilde{A}^{ij}\partial_j\alpha$$
$$+ \tilde{\gamma}^{kl}\partial_k\partial_l\beta^i + \frac{1}{3}\tilde{\gamma}^{ik}\partial_k\partial_l\beta^l + \frac{2}{3}\tilde{\Gamma}^i\partial_k\beta^k - \tilde{\Gamma}^k\partial_k\beta^i$$
$$+ 2\kappa_3\left(\frac{2}{3}\tilde{\gamma}^{ij}Z_j\partial_k\beta^k - \tilde{\gamma}^{jk}Z_j\partial_k\beta^i\right) + \beta^k\partial_k\hat{\Gamma}^i$$
$$- 2\alpha\kappa_1\tilde{\gamma}^{ij}Z_j - 16\pi\alpha\tilde{\gamma}^{ij}S_j, \quad (19)$$

$$\partial_t\alpha = -2\alpha(K - 2\Theta) + \beta^k\partial_k\alpha, \quad (20)$$

$$\partial_t\beta^i = fB^i + \beta^k\partial_k\beta^i, \quad (21)$$

$$\partial_t B^i = \partial_t\hat{\Gamma}^i - \beta^k\partial_k\hat{\Gamma}^i + \beta^k\partial_kB^i - \eta B^i, \quad (22)$$

where we have defined

$$\hat{\Gamma}^i \equiv \tilde{\Gamma}^i + 2\tilde{\gamma}^{ij}Z_j. \quad (23)$$

Note that the choice made with the definition (23) is equivalent, in the ADM context, to adding the momentum constraint to the right-hand-side of the evolution equation of $\tilde{\Gamma}^i$. In the context of the Z4 formulation, this just amounts to replacing the vector Z_i by the quantities $\hat{\Gamma}^i$ in the set of basic fields to be evolved.

The gauge conditions (20)–(22) correspond, respectively, to the standard "1 + log" slicing condition and to the original form of the gamma-driver shift condition, where a generic gauge parameter f was introduced [20]. Note that in the Z4 formulation there is an additional propagation speed and the standard BSSNOK choice of $f = 3/4$ can then lead to weak hyperbolicity when the lapse α is close to 1. This is why safer choices, such as $f = 1$, have been proposed in Ref. [28]. In this paper we use $f = 3/4$ to be as close as possible to a standard BSSNOK formulation, but we also consider how the system of equations reacts when switching to $f = 1$.

We also note that experimentation with black-hole spacetimes and the emergence of unstable behaviors, has induced us to introduce an extra parameter, κ_3, affecting some quadratic terms in the evolution Eq. (19) for $\hat{\Gamma}^i$. As discussed before, this equation corresponds to the evolution of Z_i, so this is not just a gauge choice, but rather an essential ingredient of the Z4 system. Indeed, the covariance inherent to the conformal decomposition of the Z4 system is broken unless we take $\kappa_3 = 1$. For some of the tests presented in this paper we retain a fully covariant formulation (i.e. with $\kappa_3 = 1$). However, this is not possible for black-hole spacetimes, where nonlinear couplings with the damping terms, which are important for reducing the violations in the constraints, lead to numerical instabilities. As a result, for black-hole spacetimes we have resorted to a noncovariant and conformal formulation of the Z4 system (i.e. with $\kappa_3 = 1/2$) (see discussion in Sec. III B for details).

A number of remarks are important at this point. First, although the structure of the CCZ4 formulation is very similar to the BSSNOK one, there is an important difference in the evolution of the trace-free variable $\tilde{A}_{ij}$. In the BSSNOK formulation, in fact, the Hamiltonian constraint is assumed to be satisfied *exactly* and thus used to eliminate the Ricci scalar from the right-hand-side of the evolution equation for $\tilde{A}_{ij}$ [20]. In the CCZ4 system, on the other hand, the evolution of $\tilde{A}_{ij}$ follows directly from (the trace-free part of) the original ADM evolution equation for the extrinsic curvature K_{ij}, plus the extra terms in Z_i and Θ. Second, the equivalent of the trace of the extrinsic curvature in BSSNOK formulations is given by

$$K^{\text{BSSNOK}} = K - 2\Theta, \qquad (24)$$

again because the Hamiltonian constraint is assumed to remove the Ricci scalar from the evolution equations in the BSSNOK approach. In the CCZ4 system, we rather use (the trace part of) the ADM evolution equation for K_{ij}, modulo some Z_i and Θ terms.

A closer look at the resulting CCZ4 system shows that it is not fully equivalent to the Z4 system, modulo a rearrangement of the dynamical fields. There are two extra fields which were not present in the Z4 system, namely $\det\tilde{\gamma}_{ij}$ and $\text{tr}\tilde{A}_{ij}$. These are not dynamical fields at the continuum level, where the consistency constraints

$$\det\tilde{\gamma}_{ij} = 1, \qquad \text{tr}\tilde{A}_{ij} = 0, \qquad (25)$$

hold by construction. But at the discrete level, these are just two more constraints, which can be dealt with in many different ways. For instance:

(i) *Constrained approach.* We could enforce (25) at every integration step, by removing the trace of $\tilde{A}_{ij}$ and rescaling $\tilde{\gamma}_{ij}$ as it is usually done in BSSNOK codes [34]. The remaining dynamical modes have then the same characteristic structure of the original Z4 system. This is the safest choice, and we will use it in the tests presented in this paper.

(i) *Relaxed approach.* We could instead relax (25), enforcing it just on the initial/boundary data. In this way the two extra dynamical modes propagate along normal lines, as their evolution equations [i.e. the trace of Eqs. (14) and (15)] are trivial. Note that in this case the trace of the first term in the evolution Eq. (14) must be removed explicitly to avoid any spurious numerical modes by evolving:

$$\partial_t \tilde{\gamma}_{ij} = -2\alpha\left(\tilde{A}_{ij} - \frac{1}{3}\tilde{\gamma}_{ij}\tilde{A}_{kl}\tilde{\gamma}^{kl}\right) + 2\tilde{\gamma}_{k(i}\partial_{j)}\beta^k$$
$$- \frac{2}{3}\tilde{\gamma}_{ij}\partial_k\beta^k + \beta^k\partial_k\tilde{\gamma}_{ij}.$$

Moreover, in tests like the robust stability or the gauge waves, it may be necessary to keep also under control the trace of $\tilde{A}_{ij}$. This can be achieved by adding, for instance, a damping term proportional to $\tilde{\gamma}_{ij}\text{tr}\tilde{A}_{ij}$ to the evolution Eq. (15).

Finally, the ADM constraints are given by

$$H = R - K_{ij}K^{ij} + K^2, \qquad (26)$$

$$M_i = \gamma^{jl}(\partial_l K_{ij} - \partial_i K_{jl} - \Gamma^m_{jl}K_{mi} + \Gamma^m_{ji}K_{ml}). \qquad (27)$$

In the results presented below we compute the constraint violations for both the BSSNOK and CCZ4 systems using the ADM quantities computed from the evolution variables corresponding to the two systems, allowing for the correspondence (24).

III. NUMERICAL RESULTS

In this section we validate the robustness and accuracy of the CCZ4 evolution system and compare it against the

BSSNOK system in two different cases: the gauge-waves test and black-hole spacetimes. In addition, we have performed several evolutions with the robust-stability test to ensure that the system is stable to linear perturbations, recovering the expected results (see [35] for a discussion of this test).

The numerical setup used in the simulations presented here is the same one discussed in Ref. [36] and more recently applied to the Llama code described in Ref. [37]. The latter makes use of higher-order finite-difference algorithms satisfying the summation-by-parts rule (up to 8th order in space) and a multiblock structure for the outer computational domain. More specifically, we use a central cubical Cartesian patch containing multiple levels of adaptive mesh refinement with higher-resolution boxes. The Cartesian grid is surrounded by 6 additional patches with the grid points arranged in a spherical-type geometry, with constant angular resolution to best match the resolution requirements of radially outgoing waves. This allows us to move the outer boundary to a radius where it is causally disconnected from the binary at a tiny fraction of the computational cost which would be necessary to achieve the same resolution with a purely Cartesian code. The time evolution is based on the method-of-lines with a 4th order Runge-Kutta algorithm. Our general computational infrastructure is based on the Cactus framework and we are using packages such as TwoPunctures [38], AHFinderDirect [39] and of SummationByParts [40], which are freely available and part of the Einstein Toolkit. In addition, our evolutions make use of the mesh-refinement driver Carpet [41], which implements higher-resolution boxes with multiple levels of adaptive mesh refinement.

A. Gauge waves

A classical test for different formulations of the Einstein equations is offered by the "gauge-wave" [35], in which a fictitious one-dimensional pulse propagating along the x-direction can be simulated by performing a conformal transformation of the Minkowski metric in the two-dimensional sector spanned by the (t, x) coordinates, namely, using the line element

$$ds^2 = h(x, t)(-dt^2 + dx^2) + dy^2 + dz^2. \quad (28)$$

The solution of the pulse at any time is just given by the advection of the initial profile of the gauge wave, which can be set to be smooth and periodic by choosing a sine-like initial data of the type [35]

$$h(x, t = 0) = 1 - A \sin\left(\frac{2\pi x}{L}\right), \quad (29)$$

with an amplitude $A < 1$. Although this test is apparently trivial as it does not involve the solution of the Einstein equations in a very nonlinear regime, it nevertheless

represents a serious benchmark even for formulations as robust as BSSNOK, which indeed does not pass it [42].

Following [42], we choose an amplitude of $A = 0.1$ in a domain of $L = 1$ with three uniform resolutions $h_0/L = \{1/50, 1/100, 1/200\}$ and periodic boundary conditions. Notice that the metric form (28) corresponds to an harmonic slicing condition with zero shift, so we have to change our preferred coordinate choice (i.e. the $1 + \log$ slicing with the Gamma-driver) to perform this test. Furthermore, different implementations of the CCZ4 formulation: one in which the constraints are *damped* with coefficients $\kappa_1 = 1/L$ and $\kappa_2 = 0$, and one in which the constraints are *undamped*, i.e. $\kappa_1 = 0 = \kappa_2$. We will refer to these two cases as to "Z4d" and "Z4u", respectively, (Note that in these tests the shift is set to zero and hence we do not need to specify a value for κ_3, which we take to be one).

The infinity-norm of the Hamiltonian constraint relative to simulations at the highest resolution is displayed in Fig. 1 for the damped CCZ4 formulation (black solid line), for the undamped CCZ4 formulation (blue dashed line), and for the BSSNOK formulation (red dotted line). Clearly, the BSSNOK and the CCZ4 formulation without damping terms fail before 50 crossing times (BSSNOK after 42 crossing times and Z4u after 56 crossing times) as indicated by the an exponential increase in the violation of the energy constraint. However, with the addition of the damping terms, the CCZ4 formulation is able to accurately evolve this solution for more than 1000 crossing times, while preserving the profile of the pulse. Furthermore, we have verified that the evolved solution converges to the expected spatial-discretization order (i.e. either 4th or 8th
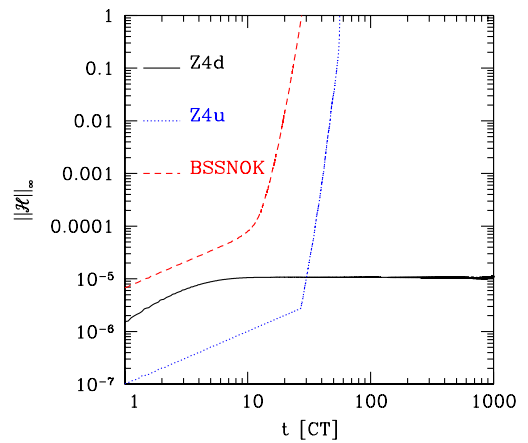

FIG. 1 (color online). L-infinity norm of the Hamiltonian constraint in the gauge-wave test, when performed with a CCZ4 formulation with damping terms (black solid line), with a CCZ4 formulation without damping terms (blue dotted line), or with the BSSNOK formulation (red dashed line). Clearly, the Z4u and the BSSNOK formulations are unstable (cf. Fig. 5 of Ref. [42]) and a similar behavior will be encountered also in black-hole spacetimes (cf. Figure 4).

order), with only a very small phase error when using the 8th order scheme.

Overall, this test shows that the dynamical control of the energy constraint via the damping term κ_1 is *crucial* to attain a stable evolution, even in such a simple type of spacetimes. We also note that this test is more demanding for conformal formulations, where there is more than one component of the metric which is nontrivial. This is confirmed by comparing our results with those in Ref. [43], where the standard Z4 formulation, i.e. not implementing a conformal decomposition, was able to pass this test without the need of damping terms. The GH formulation also passes this test.

B. Black-Hole spacetimes

Before considering black-hole binaries, we have tested extensively our new CCZ4 formulation in the evolution of single nonspinning black holes. This has allowed us to determine how different choices for the damping coefficients κ_1 and κ_2 influence the solution and, in particular, the violation of both the ADM and the Z_μ constraints. In this way we have concluded that most of the dynamics in the evolution of the constraint equations comes from the first damping coefficient, so that $\kappa_2 = 0$ represents a sensible choice and is the one that we will consider hereafter. On the other hand, increasing values of κ_1 produce lower violations of the constraints and a value of $\kappa_1 \approx 0.1/M$ seems optimal in this sense. Higher values, in fact, lead only to marginal improvements of the solution, but also tend to increase the stiffness of the damping terms.

An important and unexpected result obtained when implementing the CCZ4 formulation in black-hole spacetimes is that subtle and nonlinear couplings can occur, leading to unstable evolutions also for those choices of the coefficients that are perfectly stable in other spacetimes. While, in fact, we have carried out stable evolutions of the robust-stability test with the covariant and damped CCZ4 formulation (i.e. with $\kappa_3 = 1$ and $\kappa_1 \neq 0$), we were not able to obtain stable evolutions of black-hole spacetimes with $\kappa_3 = 1$, although the growth time of the instability does change with the values of κ_1 (see discussion around Fig. 4). Clearly, nontrivial couplings seem to appear between these coefficients, which depend on the degree of nonlinearity and which deserve further investigation to be properly understood.

On the whole, and as we will detail below, we have found that *accurate* and *stable* evolutions of binary black-hole spacetimes can be obtained with the damped noncovariant Z4 systems (i.e. with $\kappa_3 = 1/2$, $\kappa_1 = 0.1/M$). On the other hand, covariant and conformal Z4 formulations that are either damped (i.e. with $\kappa_3 = 1$, $\kappa_1 \neq 0$), or undamped (i.e. with $\kappa_3 = 1$, $\kappa_1 = 0$), have been found to lead to *unstable* evolutions, although on rather different timescales and with variable degree of accuracy (see discussion below).

The initial data of the binary black-hole evolutions is obtained from a circular-orbit condition at the third post-Newtonian order [44] and corresponds to an equal-mass nonspinning binary with an initial coordinate separation of $D = 8M$. The binary performs about 3.5 orbits before merging and settles to an isolated spinning black hole after $t \approx 360M$. To carry out a meaningful comparison, the binary is evolved with the BSSNOK and the CCZ4 formulations keeping the same choice for the gauges, namely, the $1 + \log$ slicing condition and the Gamma-driver shift condition with $f = 3/4$, $\eta = 2/M$, and the same grid setup. For the latter, in particular, we have considered three different choices aimed at determining the influence of the outer boundaries on the quality of the solution. This is a point discussed in Refs. [28,29], where it was argued that the Z4c formulation is more sensitive than the BSSNOK one to incorrect (or constraint-violating) boundary conditions. As a result, we consider three different classes of simulations depending on the treatment of the outer boundary: (i) multiblock padding and spherical outer boundary which is causally disconnected (i.e. at $\sim 2200M$ for a simulation lasting $\sim 800M$); (ii) multiblock padding and spherical outer boundary which is causally connected (i.e. at $\sim 350M$); (iii) Cartesian outer boundary which is causally connected (i.e. at $\sim 200M$). For case (i) we reduce the order of the finite-difference operator at the outer boundary but, because it is causally disconnected, the initial conditions are preserved there. For case (ii) instead, we impose reflecting boundary conditions so as to "stress" the solution with data from the outer boundary which is constraint-violating and injected mostly at the time of the reflection. Finally, in case (iii) we have applied ordinary, outgoing Sommerfeld boundary conditions to all variables, again triggering violations in the constraint equations.

All the properties of the grid structure and the treatment of the outer boundary are summarized in Table I, where h_0 is the grid spacing on the coarsest Cartesian grid, which is equal in all cases to the radial grid spacing in the angular patches. N_{ang} is the number of cells in the angular directions in the angular patches, while R_{in} and R_{out} are the inner and outer radii of the angular patches, respectively. (In the case of a Cartesian outer boundary, R_{out} represents the distance to the outer boundary along coordinate lines.) Finally, N_{lev} is the number of refinement levels (including the coarsest) on the Cartesian grid, while $2r_{\text{lev}}$ indicates the size of the cubical refinement boxes centered on each black hole.

As final remark before discussing the results, we note that all the rest being the same, at any given resolution the CCZ4 system has a smaller violation of the constraints than the BSSNOK one. At the same time, however, because the violations of both the energy and momentum constraints are part of the evolution equations in the CCZ4 system, the latter is more strongly affected than BSSNOK one, for which only the violations of the momentum constraint

TABLE I. Properties of the black-hole binaries simulated. The first column indicates the type of outer boundary and whether causally connected. h_0 is the grid spacing on the coarsest Cartesian grid, which is equal in all cases to the radial grid spacing in the angular patches. N_{ang} is the number of cells in the angular directions in the angular patches. R_{in} and R_{out} are the inner and outer radii of the angular patches. N_{lev} is the number of refinement levels (including the coarsest) on the Cartesian grid, and $2r_{lev}$ indicates the size of the cubical refinement boxes centered on each black hole. The unit of the spacetime mass M is chosen such that each black hole has mass $0.5M$ in both the single and binary black cases. Finally, the last three columns contain the relative difference in the $\ell = m = 2$ gravitational-wave phase between evolutions carried out with either the BSSNOK formulation (ϕ_B), the CCZ4 formulation with damping terms (ϕ_{Z4d}), or the CCZ4 formulation without damping terms (ϕ_{Z4u}).

outer boundary	h_0/M	N_{ang}	R_{in}/M	R_{out}/M	N_{lev}	r_{lev}/M	$(1 - \phi_{Z4d}/\phi_B)$	$(1 - \phi_{Z4u}/\phi_B)$	$(1 - \phi_{Z4d}/\phi_{Z4u})$
multiblock, caus. discon.	0.80	33	40.00	2192.80	6	(12, 6, 3, 1.5, 0.6)	0.0445	0.0465	0.00230
multiblock, caus. discon.	0.60	43	39.60	2192.40	6	(12, 6, 3, 1.5, 0.6)	0.0315	0.335	0.00175
multiblock, caus. discon.	0.48	53	39.84	2192.16	6	(12, 6, 3, 1.5, 0.6)	0.0245	0.0255	0.00135
multiblock, caus. discon.	0.40	65	40.00	2192.40	6	(12, 6, 3, 1.5, 0.6)	-	-	-
multiblock, caus. con.	0.60	43	39.60	350.40	6	(12, 6, 3, 1.5, 0.6)	-	-	-
Cartesian, caus. con.	1.20	0	-	199.20	7	(110, 12, 6, 3, 1.5, 0.6)	-	-	-

are included in the evolution system. As a result, the CCZ4 formulation requires a comparatively higher minimum-resolution treshold in order to enter a convergent regime.

A first comparison of the behavior of the different formulations is offered in Fig. 2, where we show the $\ell = m = 2$ mode of the gravitational waveform Ψ_4 as extracted on a sphere of coordinate radius $r = 100M$ (see [37] for details on the extraction procedure). Different lines refer to simulations using either the noncovariant formulation with damping terms, i.e. with $\kappa_3 = 1/2$ and $\kappa_1 = 0.1/M$, $\kappa_2 = 0$ (Z4d, black solid line), or to the noncovariant formulation without damping terms, i.e. with $\kappa_3 = 1/2$

FIG. 2 (color online). Real part of the $\ell = m = 2$ mode of the gravitational waveform Ψ_4 for an equal-mass nonspinning black-hole binary. Different lines refer to evolutions with the noncovariant formulation with and without damping terms, i.e. with $\kappa_3 = 1/2$ and $\kappa_1 = 0.1/M$, $\kappa_2 = 0$ (Z4d), or $\kappa_3 = 1/2$ and $\kappa_1 = \kappa_2 = 0$ (Z4u). The two evolutions are indicated, respectively, as Z4d and with a black solid line or as Z4u and with a blue dotted line; the BSSNOK formulation is shown with a red dashed line. Shown in the inset is a magnification of the merger.

and $\kappa_1 = \kappa_2 = 0$ (Z4u, blue dotted line). Also shown as a reference is a simulation with the BSSNOK formulation (red dashed line) using the same numerical setup. The simulations refer to the highest resolution (i.e. $h_0/M = 0.48$) and the grid having the multiblock padding and an outer boundary at $R_{out} = 2192.16$ M.

The first obvious thing to note is that all simulations lead to a stable merger and ringdown at all the resolutions considered. Furthermore, while a small phase difference is present between the Z4 and the BSSNOK runs, this difference is very small and $\Delta\phi \lesssim 0.02$ rad over the whole simulation. As a comparison, the phase difference between the Z4 and the Z4u simulations is $\Delta\phi \lesssim 0.002$ rad (see Table I for the relative maximum differences).

Although the phase differences between the waveforms obtained with the two formulations is relatively small, it also decreases with the resolution, thus indicating that both formulations would yield the same phase evolution in the continuum limit. The rate of convergence, however, is different when considering either the BSSNOK or the CCZ4 formulation. This is shown in Fig. 3, where we report the residuals in the phase evolutions at the high, medium and low resolutions, respectively (these are indicated as "HR", "MR" and "LR"). The differences between the low and medium resolutions are also scaled to highlight the convergence order of the solution. More specifically, the HR, MR and LR refer to simulations with the coarsest resolutions of $h_0/M = 0.6$, 0.48, 0.4 (cf. Table I). The convergence coefficients corresponding to these resolutions and used for rescaling are CF4 = 3.0898, CF4 = 3.0898 of 4.5 in the BSSNOK case, and CF8 = 7.1906 for a convergence factor of 8.5 in the Z4d case. Note however that, as mentioned above, the CCZ4 formulation needs a higher resolution to enter the convergence regime, while a triplet of resolutions with $h_0/M = 0.8$, 0.6, 0.48 would be enough to show convergence at about 4th order for the BSSNOK runs.
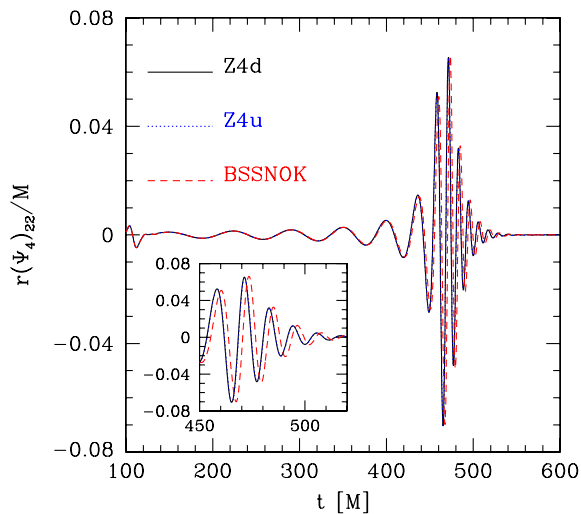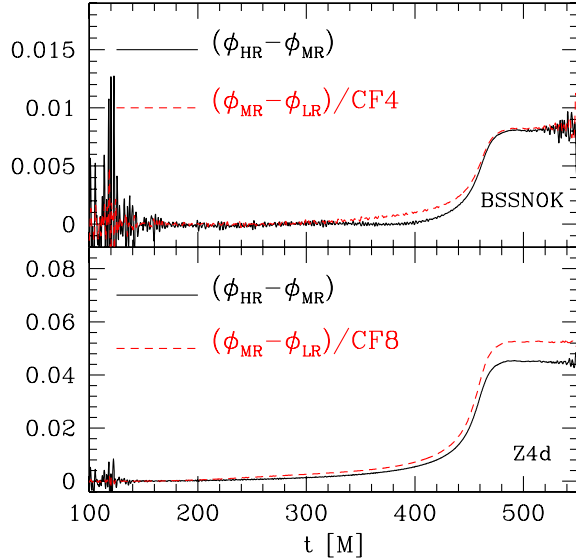
FIG. 3 (color online). Differences in the phase evolutions at the high, medium and low resolutions, respectively, (these are indicated as HR, MR and LR). The top panel refers to the BSSNOK formulation, while the bottom one the the noncovariant damped CCZ4 formulation (Z4d). The differences between the low and medium resolutions are also scaled with the appropriate convergence coefficients (marked as CF4 and CF8, see text) to highlight the convergence order of the solution; all the data refers to simulations with a multiblock padding and causally disconnected outer boundary. Note that at these resolutions the CCZ4 formulation has larger phase errors, but due its higher convergence factor, these errors are expected to decay at a faster rate than for BSSNOK.

Beside this minimum resolution threshold, the additional computational expenses required by the CCZ4 formulations are not significant. The difference with the BSSNOK system consists in an additional evolution equation for the scalar variable Θ, which would amount to solving 25 evolution equations (instead of 24 as in BSSN), implying around 4% higher computational costs. However this is an over-estimate, as in reality the time spent in computing the evolution equations depends on the computational infrastructure. In our case, it is about half of the total time of a binary black-hole simulation, while the other half is dedicated to mesh-refinement, gravitational-wave extraction and other analysis routines.

All in all, we find that for the highest resolutions used the results of the BSSNOK runs converge at about 4th order (top panel in Fig. 3), while the Z4d runs converge at about 8th order (bottom panel in Fig. 3); in both cases, the convergence order is lost in the very final stages of the merger. It is a present unclear why the two formulations yield, with the same computational infrastructure, two different convergence rates. It is possible that the constraint-damping properties of the CCZ4 formulation are able to suppress the small violations coming from the reflections across refinement boundaries, that are a major

source of error and one of the largest obstacles to attain clean convergence. However, more efforts (and considerable computational costs) need to be invested to assess whether this is the correct explanation.

A useful way to appreciate the different behavior of the two formulations is shown in Fig. 4, which reports the evolution of the L2-norm of the ADM energy (i.e. the violation of the Hamiltonian constraint) for the covariant CCZ4 formulation with and without damping (light-blue dot-dashed line and magenta long-dashed line, respectively), for the noncovariant CCZ4 formulation with and without damping (black solid line and blue dotted line, respectively), and for the BSSNOK formulation (red dashed line). We also report the different values of coefficient f in the shift Eq. (21), which does change the growth rate of the unstable simulations, but does not remove the instability in the case of the fully covariant formulation.[1] The data refers to simulations having a coarse resolution of $h_0/M = 0.48$ and outer boundary placed at $R_{\text{out}} = 2192.16$ M, but similar behaviors have been seen also at higher and lower resolutions.

Note that as the initial data settles and the evolution proceeds, the CCZ4 formulation shows a violation of the Hamiltonian constraint smaller than for the BSSNOK case (the L2-norm being at least 1 order of magnitude smaller), hence yielding a more accurate solution of the Einstein equations. However, after this initial stage, the evolutions with the CCZ4 formulation can be considerably different according to the choice made for the parameters κ_3 and κ_1. More specifically, the covariant and damped system (i.e. $\kappa_3 = 1$, $\kappa_1 \neq 0$) exhibits a very rapid violation of the constraint at $\sim 100M$ and inevitably leads to a code crash (light-blue dot-dashed line in Fig. 4). Other variants of the CCZ4 formulation, on the other hand, show a different behavior. In particular, both of the undamped CCZ4 formulations (i.e. $\kappa_3 = 1/2, 1$, $\kappa_1 = 0$) lead to a successful merger, which can be easily identifiable as the peak at about $\simeq 350$–$380M$, and which is due to larger local violations of the constraints as the merger takes place.[2] At the same time, however, both implementations show a growth of the constraint violation (blue dotted line and magenta long-dashed line). This growth can be rather slow in the case $f = 1$, but it is likely to yield unstable evolutions on very long timescales. Finally, Fig. 4 shows that a non-covariant and damped implementation of the CCZ4 formulation (i.e. $\kappa_3 = 1/2$, $\kappa_1 \neq 0$; black solid line) leads not only to a stable merger and subsequent evolution, but it

---

[1] We have performed simulations also with $\kappa_3 = 1$, $\kappa_1 = 0.1/M$, $f = 1$ or $\kappa_3 = 1$, $\kappa_1 = 0.1/M$, $f = 3/4$ and $\kappa_3 = 1$, $\kappa_1 = 0$, $f = 3/4$; in all cases we have found an instability (although with different growth rates), which we do not report to avoid overloading Fig. 4.

[2] Note that the time of merger is a gauge dependent quantity and can therefore take place at slightly different times in different formulations.
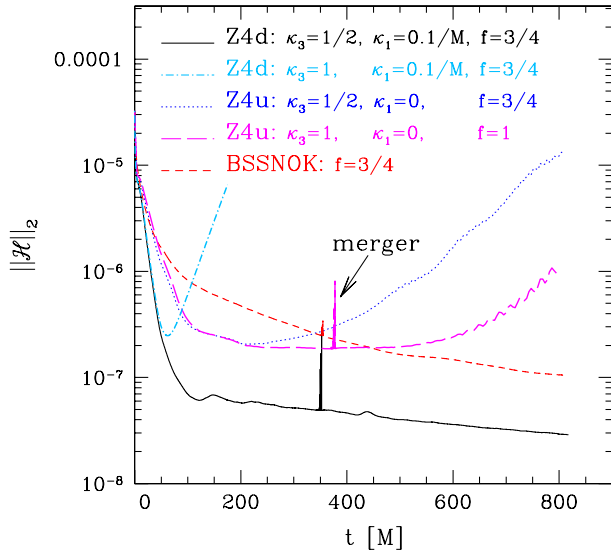
FIG. 4 (color online). L2-norm of the Hamiltonian constraint for the noncovariant CCZ4 formulation with and without damping terms (black solid line and blue dotted line, respectively), for the covariant CCZ4 formulation with and without damping terms (light-blue dot-dashed line and magenta long-dashed line, respectively), and for the BSSNOK formulation (red dashed line). Also indicated are the different values of coefficient f in the shift Eq. (21), which however do not introduce qualitatively different behaviors. The data refers to the a simulations having a coarse resolution of $h_0/M = 0.48$ and outer boundary at $R_{out} = 2192.16M$.
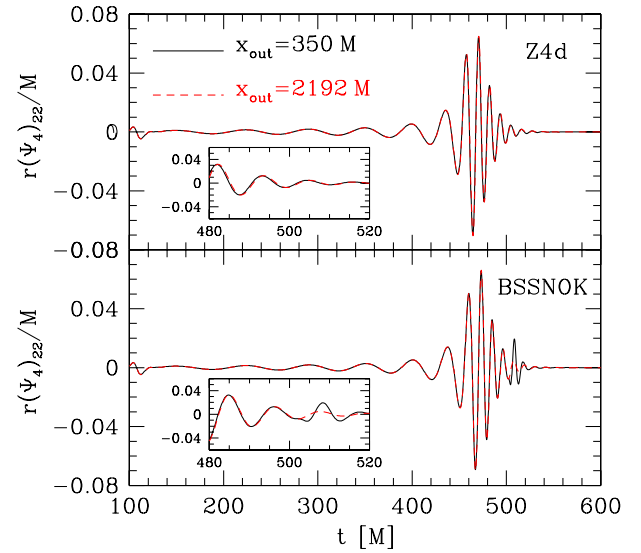

FIG. 5 (color online). Real part of the $\ell = m = 2$ mode of the gravitational waveform Ψ_4 (black solid line) extracted at $r = 100M$ for simulations having a coarse resolution $h_0/M = 0.60$ and an outer boundary which is causally connected and at $R_{out} = 350.40M$. The top panel refers to a simulation using the non-covariant and damped implementation of the CCZ4 formulation (i.e. $\kappa_3 = 1/2$, $\kappa_1 \neq 0$), while the bottom one to a simulation using the BSSNOK formulation; also shown are the corresponding waveforms obtained when $R_{out} = 2192.40M$ (red dashed lines).

also provides a violation of the constraints which is at least 1 order of magnitude smaller than the corresponding one obtained with the BSSNOK evolution (red dashed line). This is one the main results of this paper and the ultimate justification for investigating this new formulation of the equations.

We note that the behavior of the constraints described above for the CCZ4 formulation is indeed very similar to what already experienced by many groups implementing the GH formulation.[3] In that case, in fact, the addition of the damping terms was crucial to achieve stable black-hole evolutions [1,26,45]. Altogether, the evolution shown in Fig. 4 already provides the needed evidence that the new CCZ4 formulation, once suitable damping terms are added and the boundary conditions do not play a role, represents a considerable improvement over the standard BSSNOK formulation. In what follows we will show that this continues to be the case also when the outer boundaries are chosen to produce incorrect data, or when they are placed very close to the merging binary.

Figure 5 reports with black solid lines the $\ell = m = 2$ mode of the gravitational waveform Ψ_4 extracted at $r = 100M$ for simulations having a coarse resolution

---

[3]We recall that GH formulation can can be seen as a reduction of the Z4 formalism [27].

$h_0/M = 0.60$ and an outer boundary which is causally connected and at $R_{out} = 350.40M$ (cf. Table I). The top panel, in particular, refers to a simulation using the non-covariant and damped implementation of the CCZ4 formulation (i.e. Z4d, with $\kappa_3 = 1/2$, $\kappa_1 \neq 0$), while the bottom one to a simulation using the BSSNOK formulation. Also shown with red dashed lines are the corresponding waveforms obtained when the outer boundary is causally disconnected and at $R_{out} = 2192.40M$. As shown more clearly in the two insets, the CCZ4 formulation yields waveforms which are essentially identical and are unaffected by the constraint-violating outer boundaries. This is to be contrasted with the evolution performed with the BSSNOK formulation and which shows strong signs of reflection at $t \simeq 510M$.

The reason behind this different behavior is to be found in the different way in which the two formulations handle the constraint-violations coming from the outer boundaries and is best appreciated in Fig. 6, where we show again the L2-norm of the ADM energy for the noncovariant and damped implementation of the CCZ4 formulation (i.e. Z4d with $\kappa_3 = 1/2$, $\kappa_1 \neq 0$) and for the BSSNOK formulation. Note that both suffer of a very large increase at $t \sim 250M$ when the waves from the initial gauge settling of the binary, propagating at a speed of $v_g \sim \sqrt{2}$, reach the outer boundary at $R_{out} = 350.40M$ and lead to larger violations. Also note that this increase in the constraint
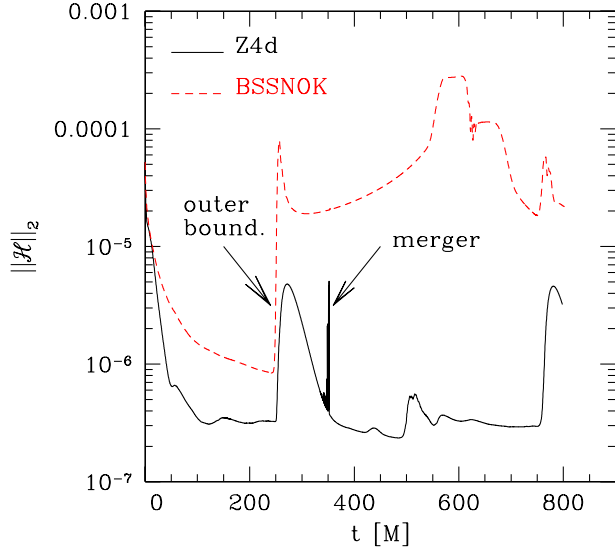
FIG. 6 (color online).   L2-norm of the Hamiltonian constraint for the noncovariant and damped implementation of the CCZ4 formulation (i.e. Z4d with $\kappa_3 = 1/2$, $\kappa_1 \neq 0$), and for the BSSNOK formulation (red dashed line). The data refers to the a simulations having a coarse resolution of $h_0/M = 0.60$ and outer boundary placed at $R_{out} = 350.40M$.
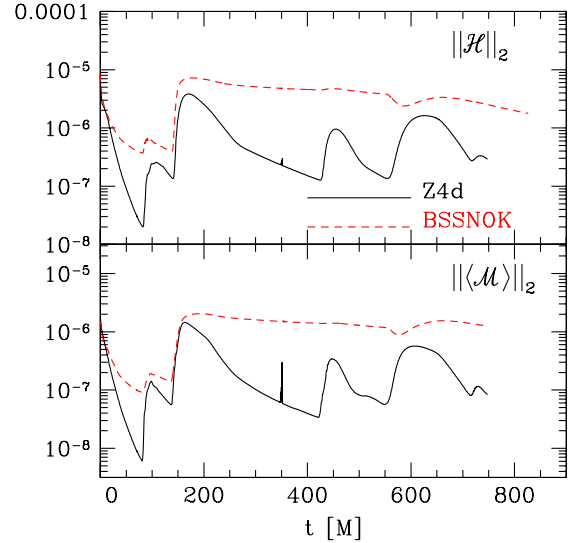

FIG. 7 (color online).   L2-norm of the Hamiltonian constraint (top panel) and of the root-mean-square of the momentum constraint (bottom panel) for the noncovariant and damped implementation of the CCZ4 formulation (i.e. Z4d with $\kappa_3 = 1/2$, $\kappa_1 \neq 0$, black solid lines), and for the BSSNOK formulation (red dashed lines). The data refers to simulations having a coarse resolution of $h_0/M = 1.20$ and outer boundary at $R_{out} = 199.20M$.

violation happens much earlier than the one associates with the merger (which is at $t \sim 350M$). As evident from Fig. 6, the CCZ4 is able to recover efficiently from this violation, and the damping terms act in such a way that by $t \sim 400M$ the violation is completely removed, with the Hamiltonian constraint brought back to its minimum value. By contrast, the evolution with the BSSNOK formulation never recovers from the boundary contamination, leading to an increasing violation responsible for the incorrect behavior discussed in Fig. 5. The CZZ4 formulation experiences another increase in the violation at $t \sim 750M$, when the gauge waves coming from the binary reach again the outer boundary, but once again the constraint damping terms act so as to remove the violation.

An additional and concluding evidence of the constraint-damping properties of the CCZ4 formulation is shown is Fig. 7, where we report the evolution of the L2-norm of the Hamiltonian constraint (top panel) and of the root-mean-square of the momentum constraint (bottom panel) for the noncovariant and damped implementation of the CCZ4 formulation (i.e. Z4d with $\kappa_3 = 1/2$, $\kappa_1 \neq 0$, black solid lines), and for the BSSNOK formulation (red dashed lines). The data refers to simulations performed with a plain Cartesian outer boundary which is very close to the binary and at $R_{out} = 199.20M$ (cf. Table I). As in the previous figure, also here it is possible to detect the increase of the constraint violations when gauge waves from the binary have reached the outer boundary at $t \sim 140M$.

Also in this case, the damping terms in the equations remove rapidly the violations, which decay exponentially to their minimum values. Because the boundary is so close-in, this behavior of rapid increase and exponential decay takes place at least 3 times, both for the Hamiltonian and momentum constraints. Any formulation of the Einstein equations having this type of behavior is obviously preferable over one in which the violations are trapped in the computational domain and are not allowed to be damped.

IV. CONCLUSIONS

By starting from the Z4 formulation [27] and by including *all* the nonprincipal terms coming from the covariant form of the equations, we have introduced the CCZ4 formulation, i.e. the conformal and covariant formulation of the Z4 system, and proposed it as a new and effective way to solve numerically the Einstein equations in arbitrary spacetimes.

The new set of equations combines the most important features of the commonly used formulations of the Einstein equations employed in numerical-relativity calculations. In particular, it is able to make use of well-tested and robust gauge conditions which remove the need of excision and, at the same time, it is able to control dynamically the violation of the constraint equations and to rapidly suppress them when they occur.

We have validated the robustness of the CCZ4 evolution system by performing a number of tests both in flat and in black-hole spacetimes. We have thus found that the CCZ4 formulation without damping terms does not pass the

standard gauge-advection test, in analogy with the behavior of the BSSNOK formulation. However, when the damping terms are switched on, the new CCZ4 formulation passes the test stably and accurately.

This ability of the formulation to control and damp violations in the constraint equations has been confirmed also through the simulation of nonspinning black-hole binaries, which have been followed for about three orbits before merging to a rapidly rotating black hole. Through a series of simulations at different resolutions and with different treatments of the outer boundary—handled either with multiblocks and placed at a causally disconnected distance, or with a Cartesian box and placed close to the binary—we have shown that *not all* of the implementations of the CCZ4 formulation lead to stable evolutions of binary black-hole spacetimes.

Rather, we have found that the covariant form of the CCZ4 formulation, in conjunction with the use of damping terms, leads to exponentially growing modes that rapidly destroy the numerical solution. Fortunately, the use of a noncovariant formulation and of damping terms leads not only to a stable evolution, but it also provides a violation of the constraints which is at least 1 order of magnitude smaller than the corresponding one obtained with the BSSNOK evolution. A close comparison with simulations performed with the BSSNOK formulation using the same numerical setup, has also revealed that the CCZ4 formulation can efficiently recover from large violations of the constraints, with the damping terms rapidly removing constraint violations produced at the outer boundary. By contrast, evolutions with the BSSNOK formulation experiencing similar violations never recover from the boundary contamination, leading to an increasing violation and incorrect gravitational waves.

Because the changes necessary to implement the new conformal formulation in BSSNOK codes and the additional computational costs are very small, we propose the new formulation as a new standard for the numerical solution of the Einstein equations in generic 3D spacetimes. We expect, in fact, that a numerical solution of the Einstein equations having smaller violations of the constraints will also yield a more accurate modelling of the gravitational-wave emission, both in vacuum and nonvacuum spacetimes.

At the same time, however, much remains to be done to fully understand the role played by the damping coefficients in fully nonlinear regimes and in the covariant form of the CCZ4 formulation. Our experience with binary black-hole spacetimes has revealed, in fact, that there are situations in which the damping of the constraints interferes negatively with a fully covariant form of the CCZ4 formulation, leading to unstable evolutions. In these cases, even small changes in the covariant character of the equations (e.g., by using $\kappa_3 = 0.9$ instead of $\kappa_3 = 1$) allows one to use nonzero damping coefficients and hence to obtain a smaller violation of the constraints. A systematic investigation of the space of parameters $\kappa_1 \times \kappa_2 \times \kappa_3$ is difficult due to the large computational costs of these simulations, but is clearly needed for a deeper understanding of the behavior of the CCZ4 formulation. Much of our future work will be dedicated to elucidate this point.

[1] F. Pretorius, Phys. Rev. Lett. **95**, 121101 (2005).
[2] M. Campanelli, C. O. Lousto, P. Marronetti, and Y. Zlochower, Phys. Rev. Lett. **96**, 111101 (2006).
[3] J. G. Baker, J. Centrella, D.-I. Choi, M. Koppitz, and J. van Meter, Phys. Rev. Lett. **96**, 111102 (2006).
[4] L. Baiotti and L. Rezzolla, Phys. Rev. Lett. **97**, 141101 (2006).
[5] T. Chu, H. P. Pfeiffer, and M. A. Scheel, Phys. Rev. D **80**, 124051 (2009).
[6] L. Baiotti, B. Giacomazzo, and L. Rezzolla, Phys. Rev. D **78**, 084033 (2008).
[7] J. Centrella, J. G. Baker, B. J. Kelly, and J. R. van Meter, Rev. Mod. Phys. **82**, 3069 (2010).
[8] M. D. Duez, Classical Quantum Gravity **27**, 114002 (2010).
[9] T. Damour and A. Nagar, Phys. Rev. D **79**, 081503 (2009).
[10] A. Buonanno *et al.*, Phys. Rev. D **79**, 124028 (2009).
[11] L. Baiotti, T. Damour, B. Giacomazzo, A. Nagar, and L. Rezzolla, Phys. Rev. Lett. **105**, 261101 (2010).
[12] C. Palenzuela, L. Lehner, and S. L. Liebling, Science **329**, 927 (2010).

[13] L. Rezzolla, B. Giacomazzo, L. Baiotti, J. Granot, C. Kouveliotou, and M. A. Aloy, Astrophys. J. **732**, L6 (2011).

[14] J. W. York, in *Sources of Gravitational Radiation*, edited by L. L. Smarr (Cambridge University Press, Cambridge, UK, 1979), pp. 83–126, ISBN 0-521-22778-X.

[15] T. Nakamura, K. Oohara, and Y. Kojima, Prog. Theor. Phys. Suppl. **90**, 1 (1987).

[16] M. Shibata and T. Nakamura, Phys. Rev. D **52**, 5428 (1995).

[17] T. W. Baumgarte and S. L. Shapiro, Phys. Rev. D **59**, 024007 (1998).

[18] H. Friedrich, Commun. Math. Phys. **100**, 525 (1985).

[19] C. Bona, J. Massó, E. Seidel, and J. Stela, Phys. Rev. Lett. **75**, 600 (1995).

[20] M. Alcubierre, B. Brügmann, P. Diener, M. Koppitz, D. Pollney, E. Seidel, and R. Takahashi, Phys. Rev. D **67**, 084023 (2003).

[21] D. Müller, J. Grigsby, and B. Brügmann, Phys. Rev. D **82**, 064004 (2010).

[22] E. Schnetter, Classical Quantum Gravity **27**, 167001 (2010).

[23] D. Alic, L. Rezzolla, I. Hinder, and P. Mösta, Classical Quantum Gravity **27**, 245023 (2010).

[24] F. Pretorius, Classical Quantum Gravity **22**, 425 (2005).

[25] L. Lindblom and B. Szilágyi, Phys. Rev. D **80**, 084019 (2009).

[26] B. Szilágyi, D. Pollney, L. Rezzolla, J. Thornburg, and J. Winicour, Classical Quantum Gravity **24**, S275 (2007).

[27] C. Bona, T. Ledvinka, C. Palenzuela, and M. Zacek, Phys. Rev. D **67**, 104005 (2003).

[28] S. Bernuzzi and D. Hilditch, Phys. Rev. D **81**, 084003 (2010).

[29] M. Ruiz, D. Hilditch, and S. Bernuzzi, Phys. Rev. D **83**, 024025 (2011).

[30] A. Weyhausen, S. Bernuzzi, and D. Hilditch, Phys. Rev. D **85**, 024038 (2012).

[31] C. Bona, C. Bona-Casas, and C. Palenzuela, Phys. Rev. D **82**, 124010 (2010).

[32] C. Gundlach, J. M. Martin-Garcia, G. Calabrese, and I. Hinder, Classical Quantum Gravity **22**, 3767 (2005).

[33] C. Bona, T. Ledvinka, C. Palenzuela, and M. Zacek, Phys. Rev. D **69**, 064036 (2004).

[34] M. Alcubierre, B. Brügmann, T. Dramlitsch, J. A. Font, P. Papadopoulos, E. Seidel, N. Stergioulas, and R. Takahashi, Phys. Rev. D **62**, 044034 (2000).

[35] M. Alcubierre, G. Allen, C. Bona, D. Fiske, T. Goodale, F. S. Guzmán, I. Hawke, S. H. Hawley, S. Husa, M. Koppitz *et al.*, Classical Quantum Gravity **21**, 589 (2004).

[36] D. Pollney, C. Reisswig, L. Rezzolla, B. Szilágyi, M. Ansorg, B. Deris, P. Diener, E. N. Dorband, M. Koppitz, A. Nagar *et al.*, Phys. Rev. D **76**, 124002 (2007).

[37] D. Pollney, C. Reisswig, E. Schnetter, N. Dorband, and P. Diener, Phys. Rev. D **83**, 044045 (2011).

[38] M. Ansorg, B. Brügmann, and W. Tichy, Phys. Rev. D **70**, 064011 (2004).

[39] J. Thornburg, Classical Quantum Gravity **21**, 743 (2004).

[40] P. Diener, E. N. Dorband, E. Schnetter, and M. Tiglio, J. Sci. Comput. **32**, 109 (2007).

[41] E. Schnetter, S. H. Hawley, and I. Hawke, Classical Quantum Gravity **21**, 1465 (2004).

[42] M. C. Babiuc *et al.*, Classical Quantum Gravity **25**, 125012 (2008).

[43] D. Alic, C. Bona, and C. Bona-Casas, Phys. Rev. D **79**, 044026 (2009).

[44] S. Husa, M. Hannam, J. A. Gonzalez, U. Sperhake, and B. Bruegmann, Phys. Rev. D **77**, 044037 (2008).

[45] F. Pretorius, Classical Quantum Gravity **23**, S529 (2006).